

From the complex plane to planet formation

Min-Kai Lin
mklin924@cita.utoronto.ca

Canadian Institute for Theoretical Astrophysics

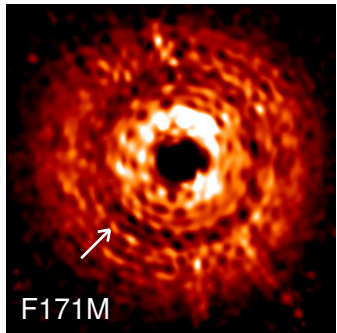
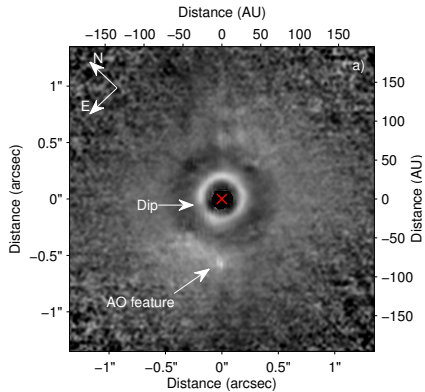
July 10 2014

Research interests

- Astrophysical fluid dynamics of accretion/protoplanetary disks
- Disk-planet interactions, orbital migration
- Self-gravitating disks
- Disk instabilities
- Magneto-hydrodynamics (new)
- Non-linear numerical simulations
- Linear hydrodynamics

Today: instabilities and large-scale structures in astrophysical disks

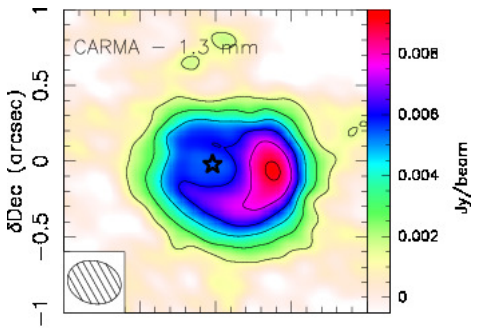
Sub-structures in protoplanetary disks



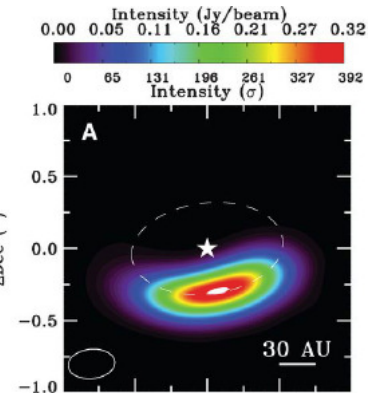
(TW Hya, Debes et al., 2013)

(HD 169142, Quanz et al., 2013)

Non-axisymmetric structures



(LkHa 330, Isella et al., 2013)

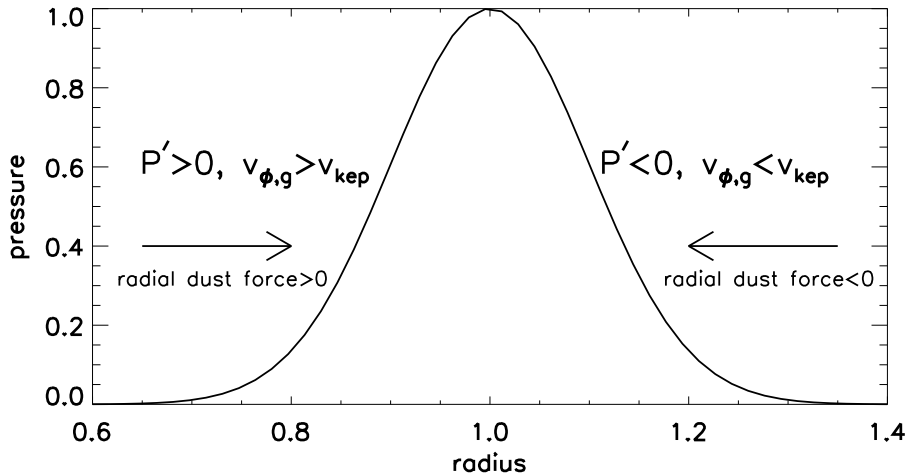


(Oph IRS 48, van der Marel et al., 2013)



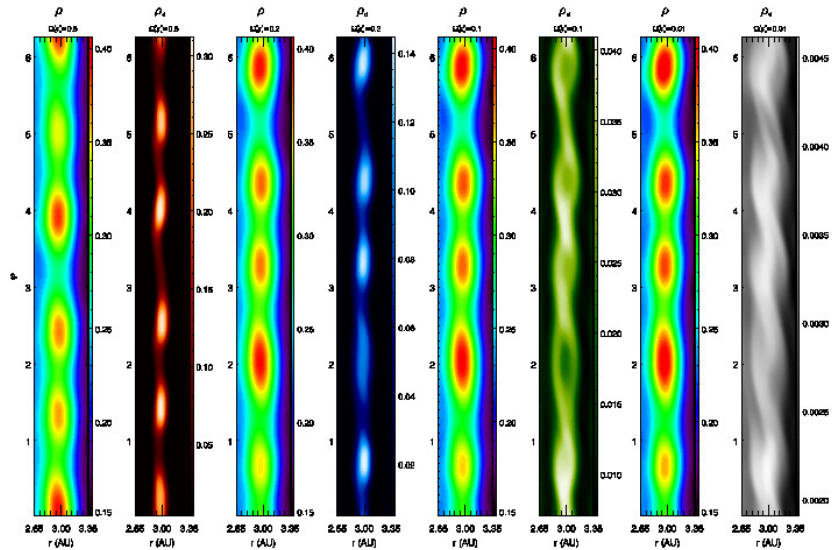
Dust-trapping

Dust trapping at pressure maxima

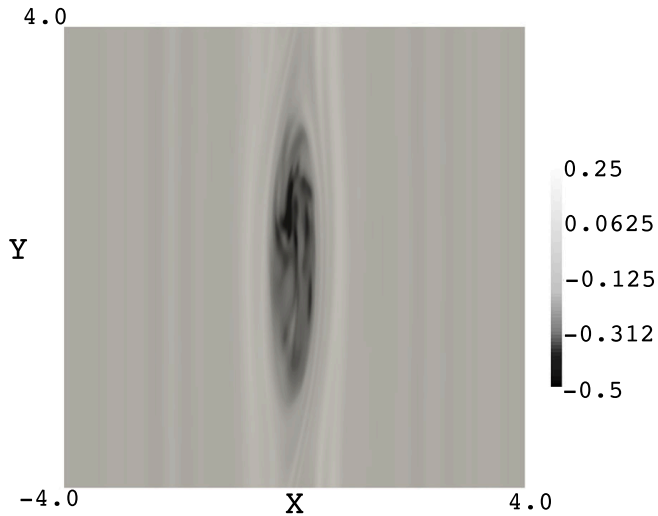


Asymmetric trapping by vortices

Meheut et al. (2012): add dust to disk with vortices



Vortex formation vs. destruction



(Lesur & Papaloizou, 2010)

Dust trapping vs. diffusion

Particle concentration vs. turbulent diffusion (Lyra & Lin, 2013)

$$\frac{\partial \rho_d}{\partial t} + \nabla \cdot (\rho_d \mathbf{v}_d) = D \nabla^2 \rho_d$$

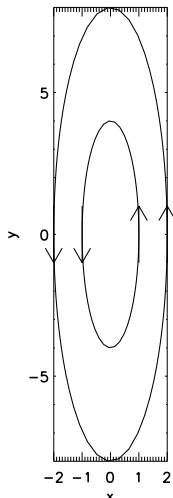
- D : from instability of vortex core
- $\mathbf{v}_d = \mathbf{v}_g + \tau c_s^2 \nabla \ln \rho_g$, isothermal gas
- \mathbf{v}_g from model of an elliptic vortex (e.g. Kida vortex)
- τ friction time

Dust plus fluid equations \rightarrow PDE for $\rho_d(x, y)$

Parameters:

$\delta = D/H^2\Omega$: dimensionless turbulence strength

$St = \tau\Omega$: dimensionless friction (Stokes number)



Steady-state dust distribution in elliptic vortices

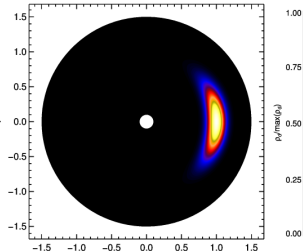
$$\rho_d(a) \propto \exp\left(-\frac{a^2}{2H_v^2}\right),$$

with

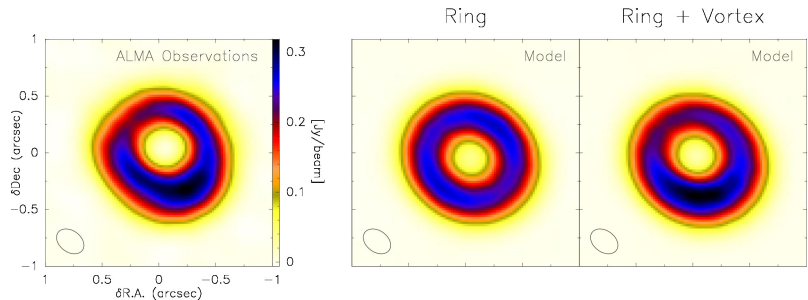
$$H_v(\chi, \delta, \text{St}) = \frac{H_g}{f(\chi)} \sqrt{\frac{\delta}{\delta + \text{St}}}.$$

Dust density averaged over an ellipse (semi-minor axis a , aspect-ratio χ)
EXACT solution for certain vortex models

(e.g. Kida vortex with $\chi = 7 \rightarrow$ no pressure gradient along ellipses)



Application to observations

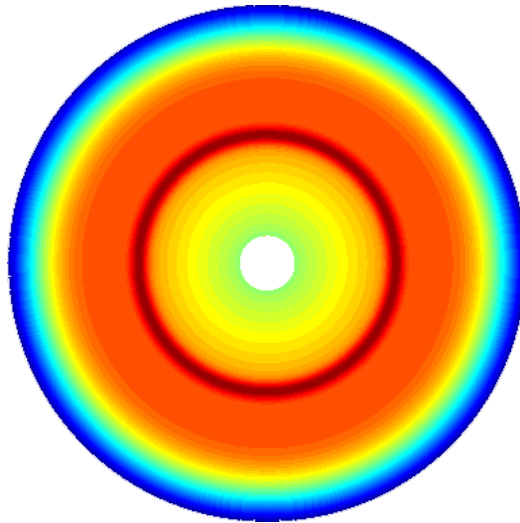


(SAO 206462, Pérez et al., 2014)

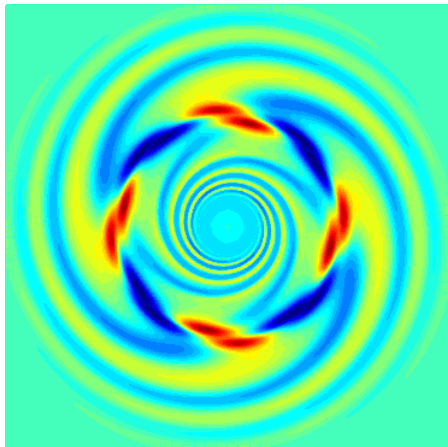
$\chi_{\text{obs}} \sim 7$, model+ data $\rightarrow v_{\text{turb}} \sim 0.22 c_s$.

Vortex formation from the Rossby wave instability

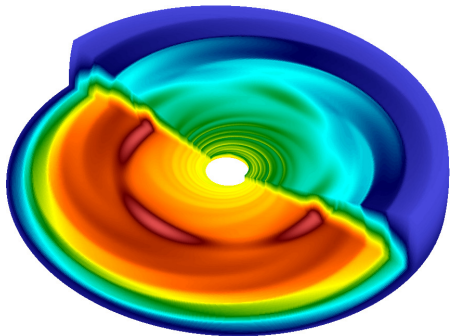
- Kelvin-Helmholtz instability in a rotating disk (Lovelace et al., 1999)
- Requires a radially-structured disk (e.g. planet gaps)



Numerical examples of the RWI



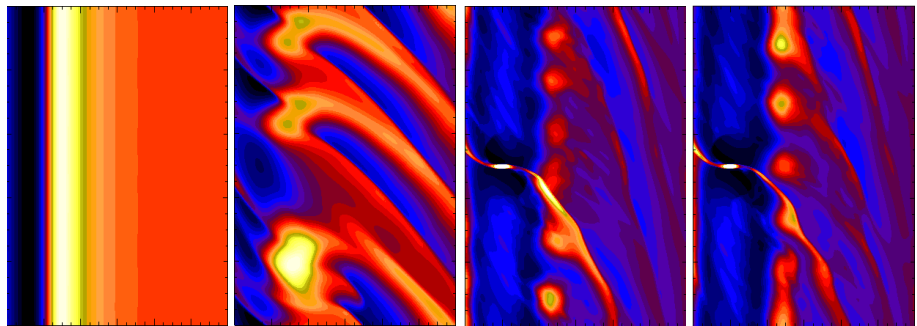
ATHENA code: 3D disk in a box



ZEUS code: 3D self-gravitating
adiabatic disk, spherical grid

Numerical examples of the RWI

PLUTO code



3D disk with viscosity jump in radius

3D self-gravitating disk-planet simulation

[Note: global simulations plotted in a box ($r \rightarrow x$, $\phi \rightarrow y$)]

Step 1: linear problem

- ① Steady, axisymmetric, vertically hydrostatic density bump at $r = r_0$
- ② Perturb fluid equations, e.g. $\rho \rightarrow \rho + \delta\rho(r, z) \exp i(m\phi + \sigma t)$
- ③ Combine linear equations to get equation for $W \equiv \delta p/\rho$:

$$L(r, z; \sigma)W = 0.$$

- $W \rightarrow$ eigenfunction ; $\sigma \rightarrow$ eigenvalue

Co-rotation singularity where $\bar{\sigma} \equiv \sigma + m\Omega = 0$,

$$L = \cdots + \frac{1}{\bar{\sigma}} \frac{d}{dr} \left(\frac{\Sigma\Omega}{\kappa^2} \right).$$

RWI: $\text{Re}[\bar{\sigma}(r_0)] \simeq 0$ and $\frac{d}{dr} \left(\frac{\Sigma\Omega}{\kappa^2} \right) \Big|_{r_0} \simeq 0$

Step 1: linear problem

- ① Steady, axisymmetric, vertically hydrostatic density bump at $r = r_0$
- ② Perturb fluid equations, e.g. $\rho \rightarrow \rho + \delta\rho(r, z) \exp i(m\phi + \sigma t)$
- ③ Combine linear equations to get equation for $W \equiv \delta p/\rho$:

$$L(r, z; \sigma)W = 0.$$

- $W \rightarrow$ eigenfunction ; $\sigma \rightarrow$ eigenvalue

Co-rotation singularity where $\bar{\sigma} \equiv \sigma + m\Omega = 0$,

$$L = \cdots + \frac{1}{\bar{\sigma}} \frac{d}{dr} \left(\frac{\Sigma\Omega}{\kappa^2} \right).$$

Pole in complex plane \rightarrow linear instability \rightarrow vortices \rightarrow dust-trapping \rightarrow planetesimal formation \rightarrow planets

Example: RWI in 3D polytropic disk ($p \propto \rho^{1+1/n}$)

Convert to 1D problem,

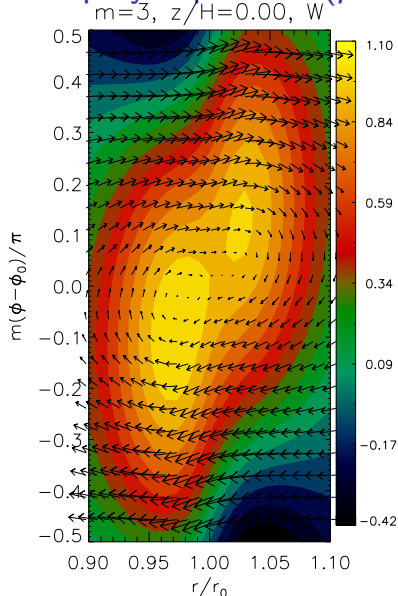
$$W(r, z) = \sum_{l=0}^{\infty} W_l(r) C_l^{\lambda}(z/H),$$

where $C_l^{\lambda}(x)$ are Gegenbauer polynomials. (Generalized Legendre/Chebyshev.)

$$L(r, z; \sigma)W = 0 \rightarrow A_l(W_l) + B_l(W_{l-2}) + C_l(W_{l+2}) = 0.$$

- Technical but neat
- No freedom in upper disk boundary conditions

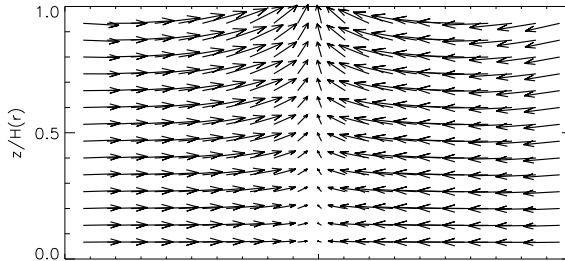
Example: RWI in 3D polytropic disk ($p \propto \rho^{1+1/n}$)



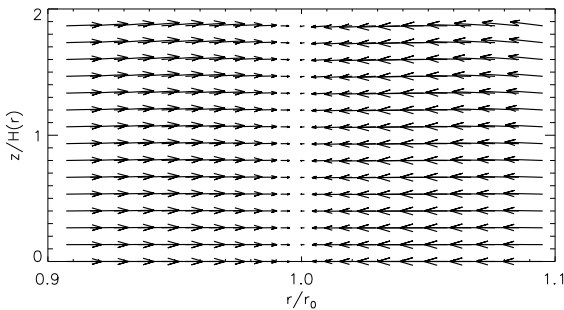
Anti-cyclonic motion associated with over-density.

Example: RWI in 3D polytropic disk ($p \propto \rho^{1+1/n}$)

Magnitude of vertical motion decreases with increasing n (more compressible)



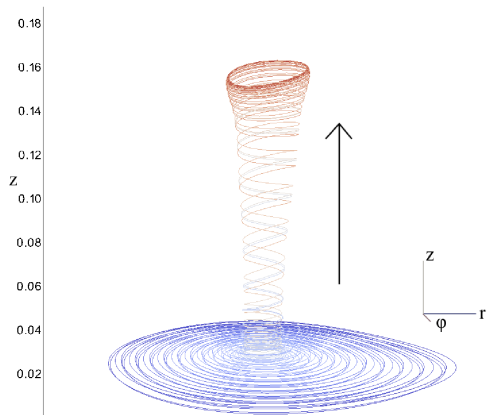
← $n = 1.0$ polytrope



← vertically isothermal disk
($n = \infty$, special treatment
with Hermite polynomials)

Comparison to non-linear simulations

Upward motion seen in non-linear hydrodynamic simulations of Meheut et al. (2012):



Meheut et al. (2012) → mm dust lifted to disk surface

Extension to adiabatic 3D disks

- $p \propto \rho^\Gamma$ in basic state only
- Energy equation $Ds/Dt = 0$, $s \equiv p/\rho^\gamma \propto \rho^{\Gamma-\gamma}$
- $\gamma \geq \Gamma \geq 1$, density bump \rightarrow entropy dip

$$V_1 W + \overline{V}_1 Q = 0$$
$$V_2 W + \overline{V}_2 Q = 0$$

- $W = \delta p / \rho \rightarrow$ pressure perturbation
- $Q = c_s^2 \delta \rho / \rho \rightarrow$ density perturbation

Finite-difference/pseudo-spectral method:

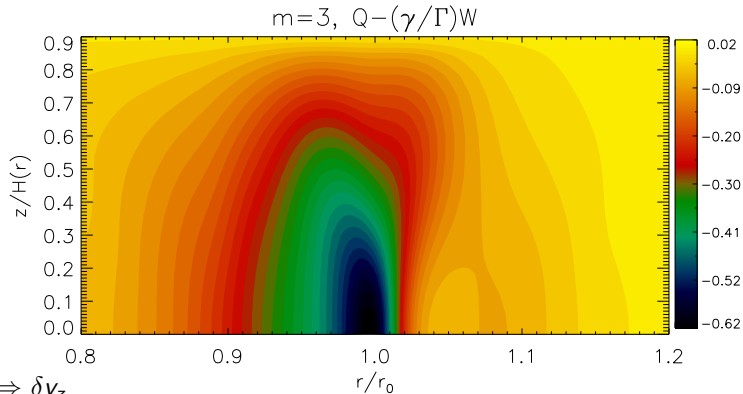
$$W(r_i, z) \equiv W_i(Z) = \sum_{k=1}^{N_z} w_{ki} \psi_k(Z/Z_{\max})$$

$[\psi_k = T_{2(k-1)}$ are Chebyshev polynomials]

Baroclinity/buoyancy, $\nabla p \times \nabla \rho \neq 0$

$$\bar{S} \equiv Q - \frac{\gamma}{\Gamma} W$$

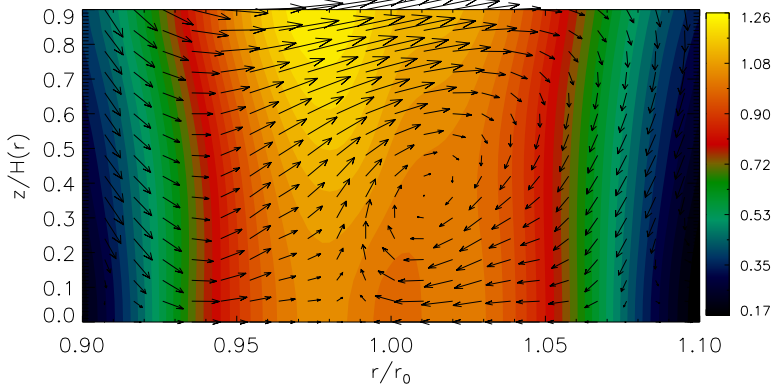
→ a measure of baroclinity ($= 0$ if $\Gamma = \gamma$)



- $\bar{S} \Rightarrow \delta v_z$
- $\nabla \bar{S} \Rightarrow (\nabla \times \delta \mathbf{v})_\phi$

Example: meridional vortical motion in adiabatic disks

$\Gamma = 1.67$, $\gamma = 2.5$, $m = 5$ along $\phi = \phi_0 - \frac{m_0}{m_1} \ln r$



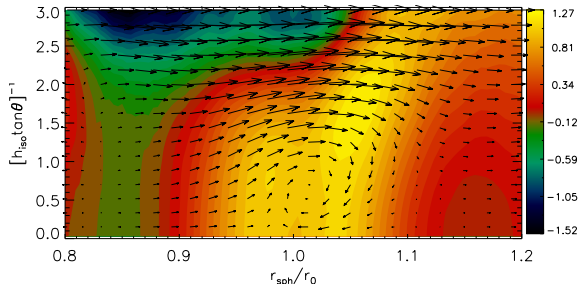
Buoyancy > pressure at large heights, since

$$\frac{\text{pressure}}{\text{buoyancy}} \sim \frac{\Omega^2}{N_z^2} \frac{\partial \ln W}{\partial \ln z},$$

and vertical frequency $N_z \rightarrow \infty$ as $z \rightarrow H$. 'Swirling' because of entropy pert.

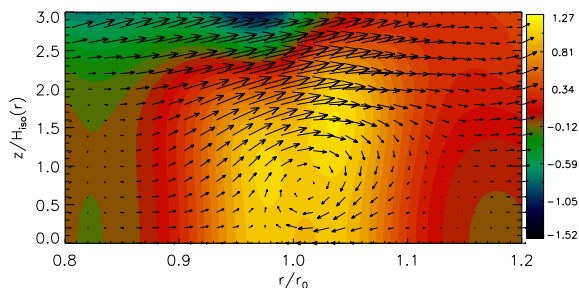
Comparison with hydrodynamic simulations

- Isothermal disk, adiabatic evolution ($\Gamma \equiv 1$, $\gamma = 1.4$)



← ZEUS simulation

$$\begin{aligned}\operatorname{Re}(\sigma) &= -0.99m\Omega_0 \\ \operatorname{Im}(\sigma) &= -0.194\Omega_0\end{aligned}$$



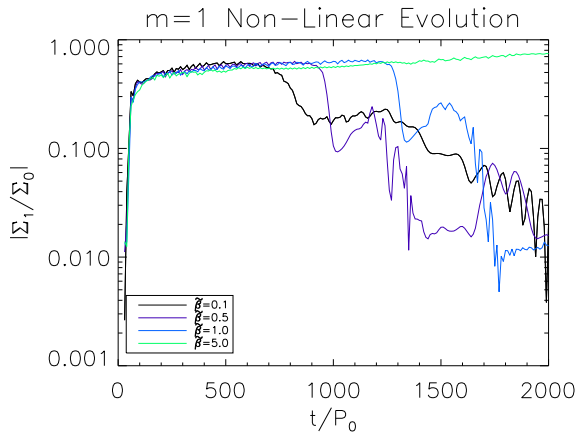
← linear code

$$\begin{aligned}\operatorname{Re}(\sigma) &= -0.9896m\Omega_0 \\ \operatorname{Im}(\sigma) &= -0.1937\Omega_0\end{aligned}$$

Gap formation and stability in non-isothermal disks

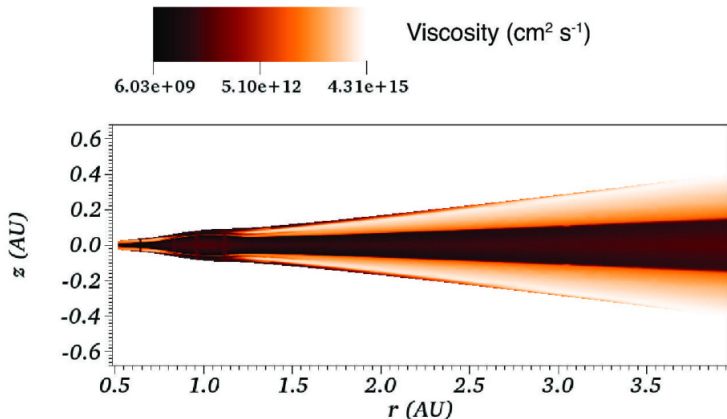
[2014 CITA Summer student program]

- FARGO 2D, disk-planet
- $t_{\text{cool}} = \tilde{\beta} \times t_{\text{libration}}$



Very long cooling actually gives *shorter* vortex lifetime (R. Les & Lin, in prep.)

Vortex-formation in layered-accretion disks?



(Axisymmetric model from Landry et al., 2013)

- RWI requires low viscosity, but only have dead zone near midplane
- Rossby vortices have weak vertical structure (vorticity columns)

Linear RWI in layered disks

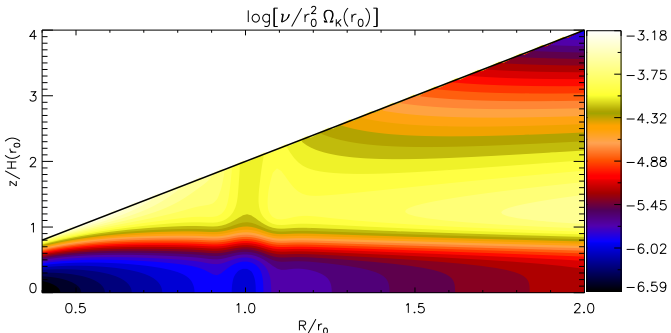
First task for any linear problem: equilibrium state. But:

- Need localized radial gradient for RWI
- Want a viscous atmosphere

Linear RWI in layered disks

First task for any linear problem: equilibrium state. But:

- Need localized radial gradient for RWI
- Want a viscous atmosphere



(Lin, 2014b)

- Choose viscosity and v_R s.t. $R\rho v_R = \dot{M}(z)$
- Strictly isothermal gas

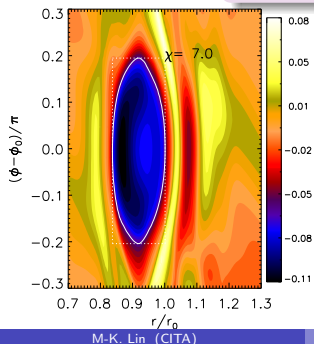
PLUTO simulations of layered disks

Spherical grid, $z \in [0, 2H]$ at $R = r_0$.

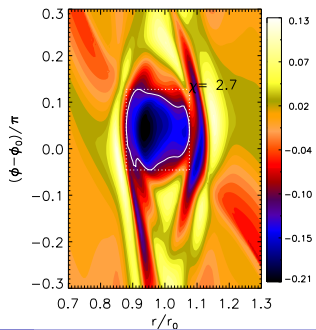
ν decreases by 10^2 from active (upper) to dead (lower) layer.

- Case 1: all dead, linear growth rate = 0.199Ω
($\alpha \sim 10^{-4}$)
- Case 2: half dead, linear growth rate = 0.182Ω
($\alpha \sim 10^{-4}$ for $z \in [0, H]$; $\alpha \sim 10^{-2}$ for $z \in [H, 2H]$)

Local viscous time $H^2/\nu \gg t_{\text{RWI}}$

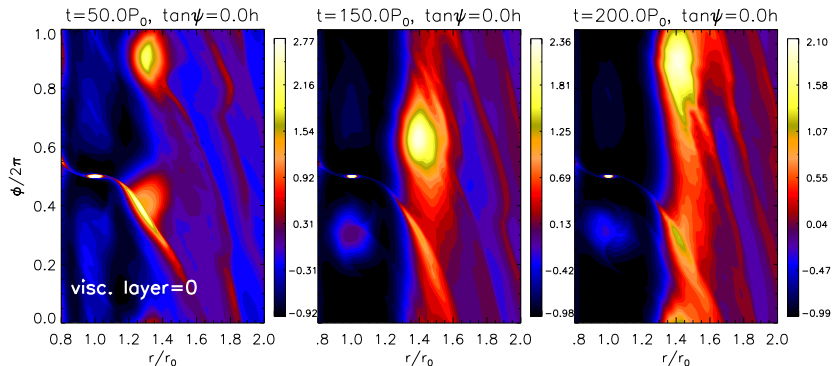


← Rossby numbers →
← Case 1
Case 2 →



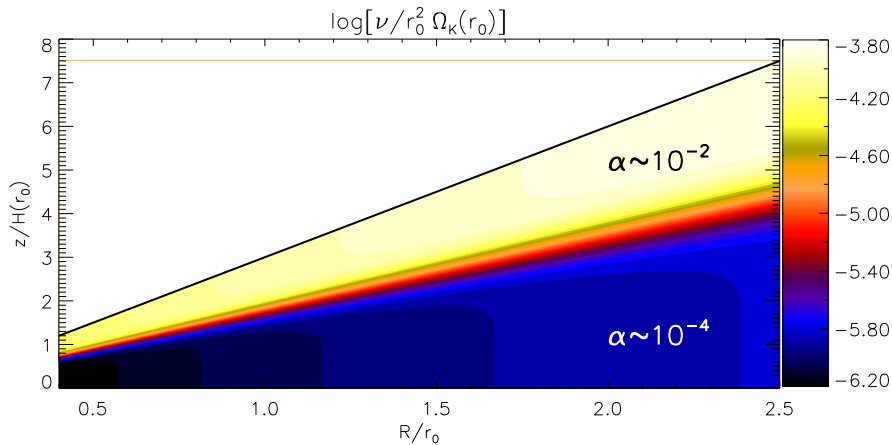
Disk-planet interaction in layered disks

Standard result for Jupiter-mass planet in a low viscosity unlayered disk
 $(\alpha \sim 10^{-4})$



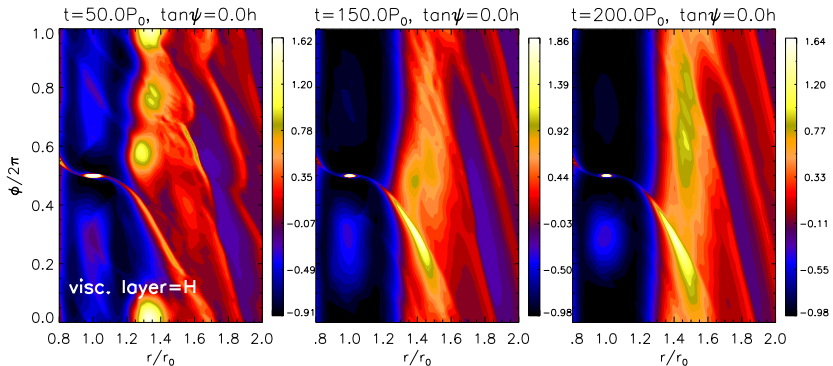
Disk-planet interaction in layered disks

Repeat simulation with layered viscosity



Disk-planet interaction in layered disks

Rossby vortex does not survive against viscous layer

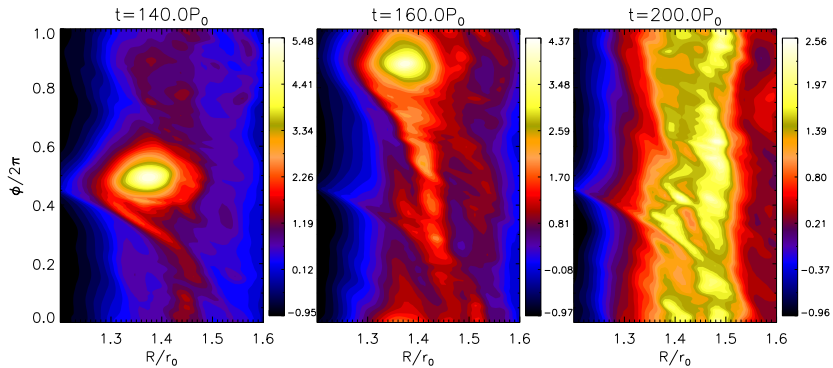


Vertical domain size: $z \in [0, 3H]$, viscous layer $z \in [2, 3H]$, $\Sigma_{\text{visc}}/\Sigma \sim 0.04$

- Lesson: long term vortex formation sensitive to disk vertical structure
- Next step: back-reaction on α

Disk-planet interaction in layered disks

Restart a low-viscosity simulation with a viscous atmosphere



Vertical domain size: $z \in [0, 3H]$, viscous layer $z \in [2, 3H]$, $\Sigma_{\text{visc}}/\Sigma \sim 0.04$

- Lesson: long term vortex formation sensitive to disk vertical structure
- Next step: back-reaction on α

Magnetized massive astrophysical disks

Principle routes to turbulent angular momentum transport in rotating disks:

Magneto-rotational instability

and

Gravitational instability

May have MRI and GI in:

- Early evolution of protoplanetary disks
- Layered accretion in PPDs
- Black hole accretion disks
- Galactic disks

Latest work in PPDs: Fromang et al. (2004) using full simulations

Step 1: linear stability (Lin, 2014a)

Shearing box resistive MHD plus Poisson, linearize →

$$\frac{i\sigma}{c_s^2} W + ik_x \delta v_x + (\ln \rho)' \delta v_z + \delta v'_z = 0,$$

$$i\sigma \delta v_x - 2\Omega \delta v_y = -ik_x \tilde{W} + \frac{B_z}{\mu_0 \rho} [\delta B'_x - ik_x (\delta B_z + \epsilon \delta B_y)],$$

$$i\sigma \delta v_y + \frac{\kappa^2}{2\Omega} \delta v_x = \frac{B_z}{\mu_0 \rho} \delta B'_y,$$

$$i\sigma \delta v_z = -\tilde{W}' - \frac{B_y}{\mu_0 \rho} \delta B'_y,$$

$$i\bar{\sigma} \delta B_x = B_z \delta v'_x + \eta \delta B''_x + \eta' \delta B'_x - ik_x \eta' \delta B_z,$$

$$i\bar{\sigma} \delta B_y = B_z \delta v'_y - B_y \Delta - S \delta B_x + \eta \delta B''_y + \eta' \delta B'_y,$$

$$i\bar{\sigma} \delta B_z = -ik_x B_z \delta v_x + \eta \delta B''_z,$$

$$\delta \Phi'' - k_x^2 \delta \Phi = \frac{\rho}{c_s^2 Q} W.$$

Pseudo-spectral method reduces numerical complexity

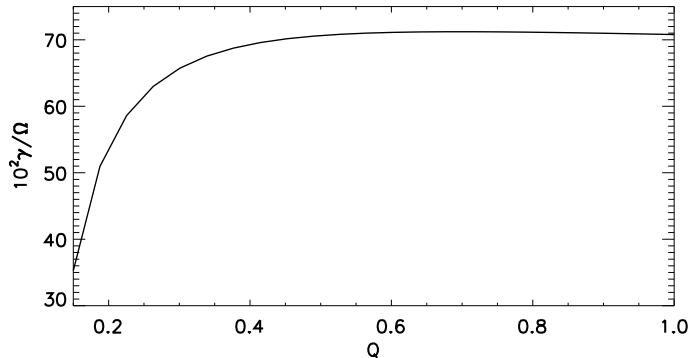
Effect of SG on the MRI through the background

Rule of thumb for MRI:

$$\lambda_{\text{MRI}} \lesssim 2H$$

$\lambda_{\text{MRI}} \sim \frac{v_A}{\Omega} = \frac{B_z}{\sqrt{\mu_0 \rho}} \frac{1}{\Omega}$, $H = H(Q)$ decreases with increasing SG

So, for fixed $\beta \equiv c_s^2/v_A^2$,



Note: $Q = 0.5 \longleftrightarrow Q_{2D} = 1.5$.

Limiting field strength

Example: polytropic disk with $p \propto \rho^2$, then $\lambda_{\text{MRI}} \lesssim 2H \rightarrow$

$$\beta^{-1/2} \lesssim \frac{\sqrt{15}}{4\pi} \sqrt{Q} \arccos \left(\frac{Q}{1+Q} \right).$$

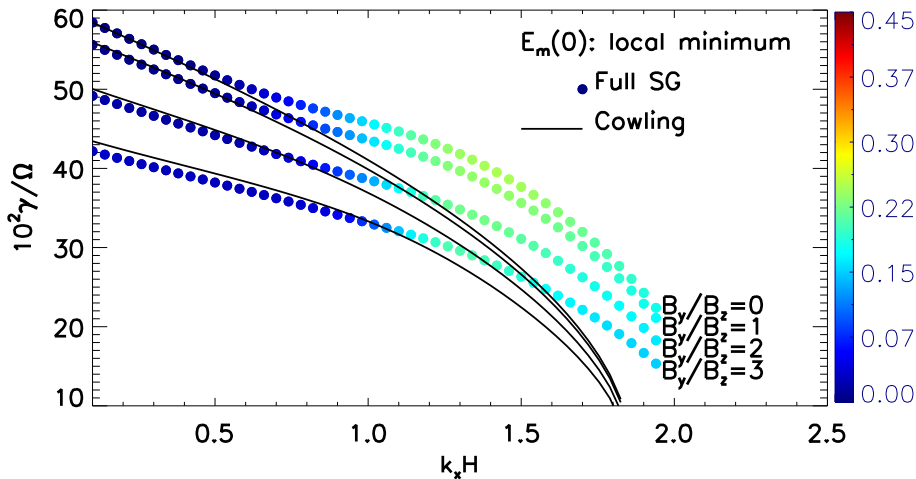
For $Q \ll 1$,

$$\frac{B_z}{c_{s0}\Omega} \sqrt{\frac{\pi G}{\mu_0}} \lesssim \frac{\sqrt{15}}{16}.$$

Both $v_A, \lambda_{\text{MRI}} \rightarrow 0$ and $H \rightarrow 0$ as $\rho(0) \rightarrow \infty$.

Effect of SG on the MRI through the perturbation

Modes with perturbed magnetic energy *minimized* at $z = 0$

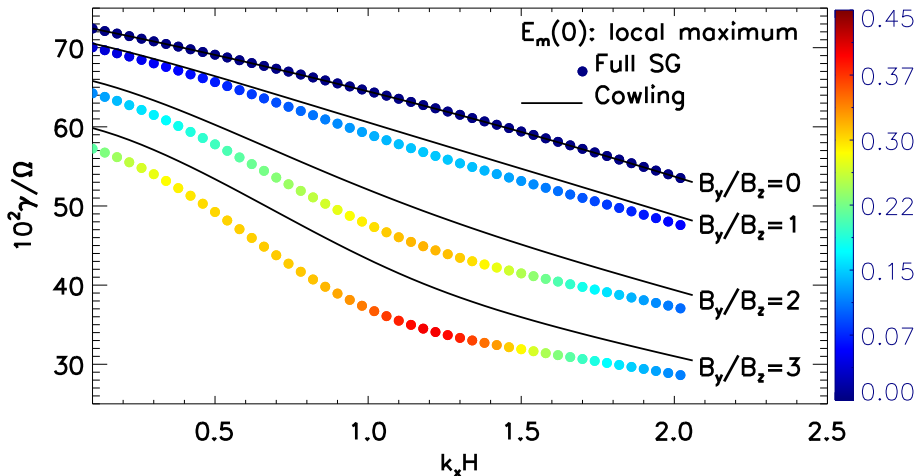


$$\delta\rho'(0) = 0 \text{ for } B_y = 0$$

Colourbar: $E_{\text{grav}} / (E_{\text{grav}} + E_{\text{mag}})$

Effect of SG on the MRI through the perturbation

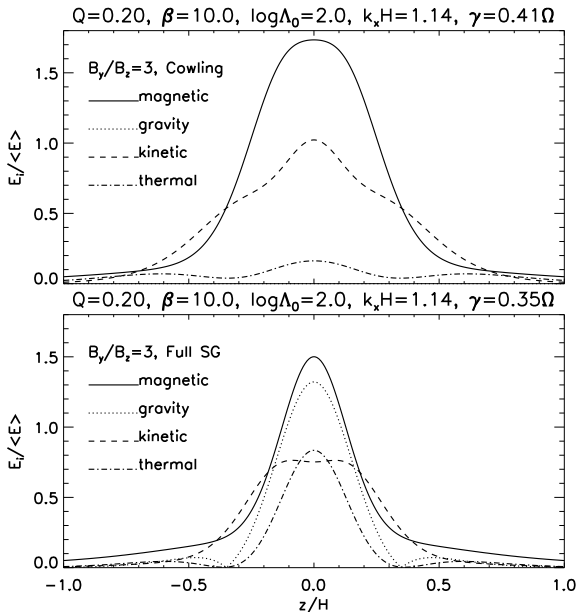
Modes with perturbed magnetic energy *maximized* at $z = 0$



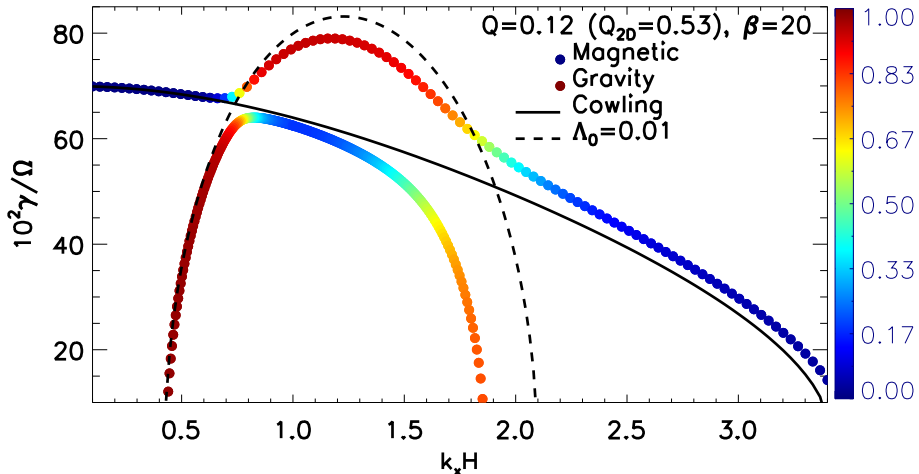
$$\delta\rho(0) = 0 \text{ for } B_y = 0$$

$$\text{Colourbar: } E_{\text{grav}} / (E_{\text{grav}} + E_{\text{mag}})$$

Effect of SG on the MRI through the perturbation



Co-existence of MRI and GI



- ‘Avoided crossing’ of modes
- MRI-GI interaction only possible with same parity

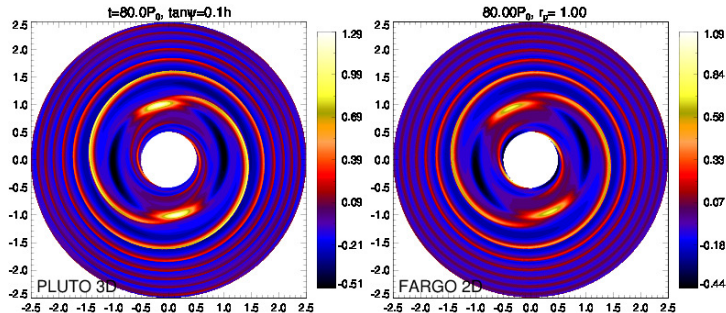
Future

Linear

Non-axisymmetric modes in magnetized self-gravitating disks

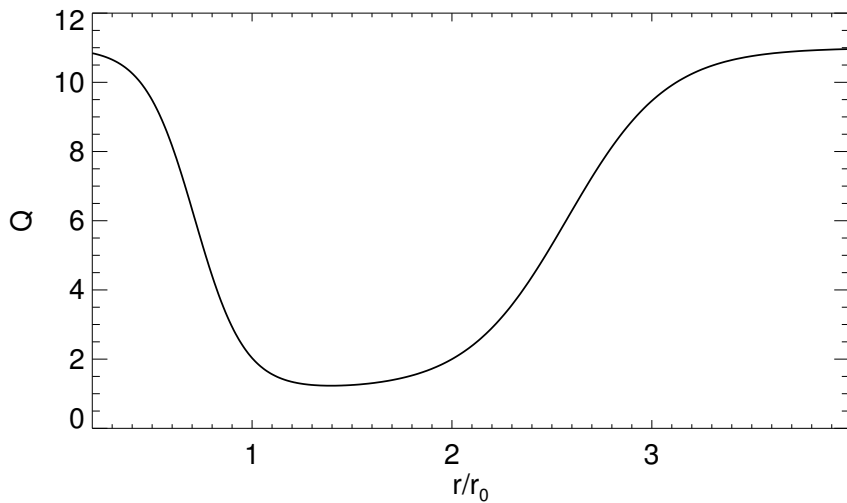
- 2D global, 3D local
- Numerically technical (integro-differential equation eigenvalue problem)
- Effect of magnetic field/MRI on angular momentum transport by gravity, global structures

3D edge instabilities with self-gravity



Future

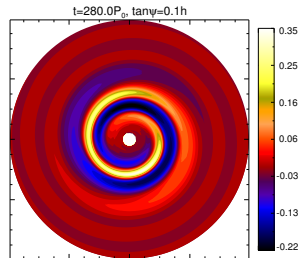
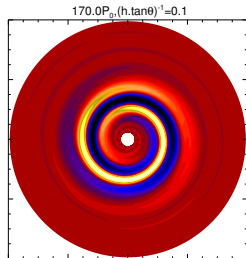
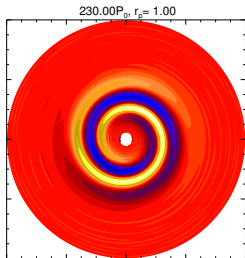
Non-linear



Future

Non-linear

Eccentric modes in radially-structured disks (?)



FARGO 2D

ZEUS 3D

PLUTO 3D

- Finite difference
- Poisson: 2D FFT

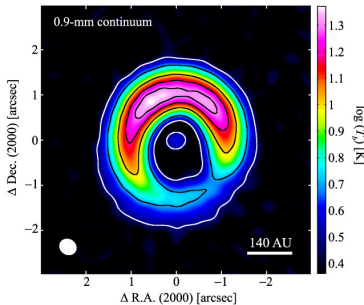
- Finite difference
- Poisson: linear solver

- Godunov
- Poisson: spherical harmonic expansion

Future

Non-linear

- Observational relevance: HD 142527



Estimated $Q \sim 1-2$ (Fukagawa et al., 2013; Christiaens et al., 2014)

- Theoretical relevance: episodic accretion
GI in dead zone \rightarrow MRI, but what kind of GI? Turbulence or large-scale waves?

References

- Christiaens V., Casassus S., Perez S., van der Plas G., Ménard F., 2014, ApJL, 785, L12
- Debes J. H., Jang-Condell H., Weinberger A. J., Roberge A., Schneider G., 2013, ApJ, 771, 45
- Fromang S., Balbus S. A., De Villiers J.-P., 2004, ApJ, 616, 357
- Fukagawa M., Tsukagoshi T., Momose M., Saigo K., Ohashi N., Kitamura Y., Inutsuka S.-i., Muto T., Nomura H., Takeuchi T., Kobayashi H., Hanawa T., Akiyama E., Honda M., Fujiwara H., Kataoka A., Takahashi S. Z., Shibai H., 2013, PASJ, 65, L14
- Isella A., Pérez L. M., Carpenter J. M., Ricci L., Andrews S., Rosenfeld K., 2013, ApJ, 775, 30
- Landry R., Dodson-Robinson S. E., Turner N. J., Abram G., 2013, ApJ, 771, 80
- Lesur G., Papaloizou J. C. B., 2010, A&A, 513, A60
- Lin M.-K., 2014a, ArXiv e-prints
- Lin M.-K., 2014b, MNRAS, 437, 575
- Lovelace R. V. E., Li H., Colgate S. A., Nelson A. F., 1999, ApJ, 513, 805
- Lyra W., Lin M.-K., 2013, ApJ, 775, 17
- Meheut H., Keppens R., Casse F., Benz W., 2012, A&A, 542, A9
- Meheut H., Meliani Z., Varniere P., Benz W., 2012, A&A, 545, A134
- Pérez L. M., Isella A., Carpenter J. M., Chandler C. J., 2014, ApJL, 783, L13
- Quanz S. P., Avenhaus H., Buenzli E., Garufi A., Schmid H. M., Wolf S., 2013, ApJL, 766, L2
- van der Marel N., van Dishoeck E. F., Bruderer S., Birnstiel T., Pinilla P., Dullemond C. P., van Kempen T. A., Schmalzl M., Brown J. M., Herczeg G. J., Matthews G. S., Geers V., 2013, Science, 340, 1199